Electronic Supplementary Material (ESI) for Journal of Materials Chemistry B.

Supporting Information for

AMF Responsive DOX-loaded Magnetic Microspheres: Transmembrane Drug Release Mechanism and Multimodality Postsurgical Treatment of Breast Cancer

Weiming Xue [b,1], Xiao-Li Liu [a,c,1], Heping Ma [b], Wensheng Xie [e], Saipeng Huang [b], Huiyun Wen [b], Guangyin Jing [d], Lingyun Zhao [e], Xing-Jie Liang [c], Hai Ming Fan [a*]

a Key Laboratory of Synthetic and Natural Functional Molecule Chemistry of the Ministry of Education, College of Chemistry and Materials Science, Northwest University, Xi'an, Shaanxi, 710069, People's Republic of China

b School of Chemical Engineering, Northwest University, Xi'an, Shaanxi, 710069, People's Republic of China

c CAS Key Laboratory for Biomedical Effects of Nanomaterials and Nanosafety, National Center for Nanoscience and Technology, Beijing, 100190, People's Republic of China

d Department of Physics, State Key Lab Incubation Base of Photoelectric Technology and Functional Materials, Northwest University, Xi'an, Shanxi, 710069, People's Republic of China

e State Key Laboratory of New Ceramics and Fine Processing, Key Laboratory of Advanced Materials, School of Material Science & Engineering, Tsinghua University, Beijing,100084, People's Republic of China

[1] These authors contributed equally to this work.

* Corresponding author: Prof. Dr. Hai Ming Fan

Tel.: +86 29 81535040; Fax: +86 29 81535040

E-mail address: fanhm@nwu.edu.cn.

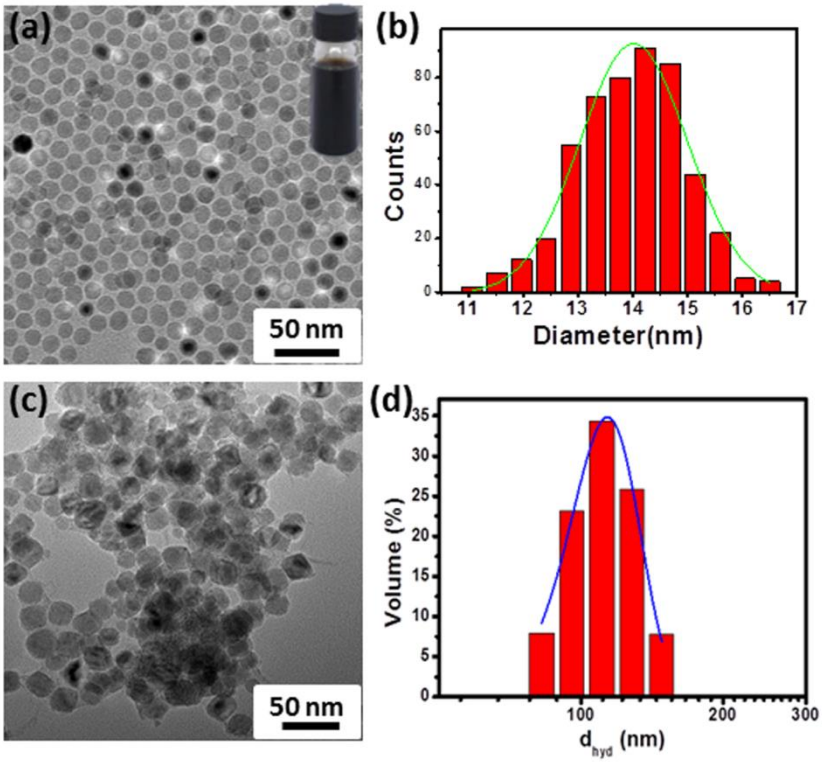

Figure S1. (a) TEM image and (b) size distribution histogram of the as-synthesized SPIONs; (c) TEM image and (d) hydrodynamic size of SPIONs after surface oxidation.

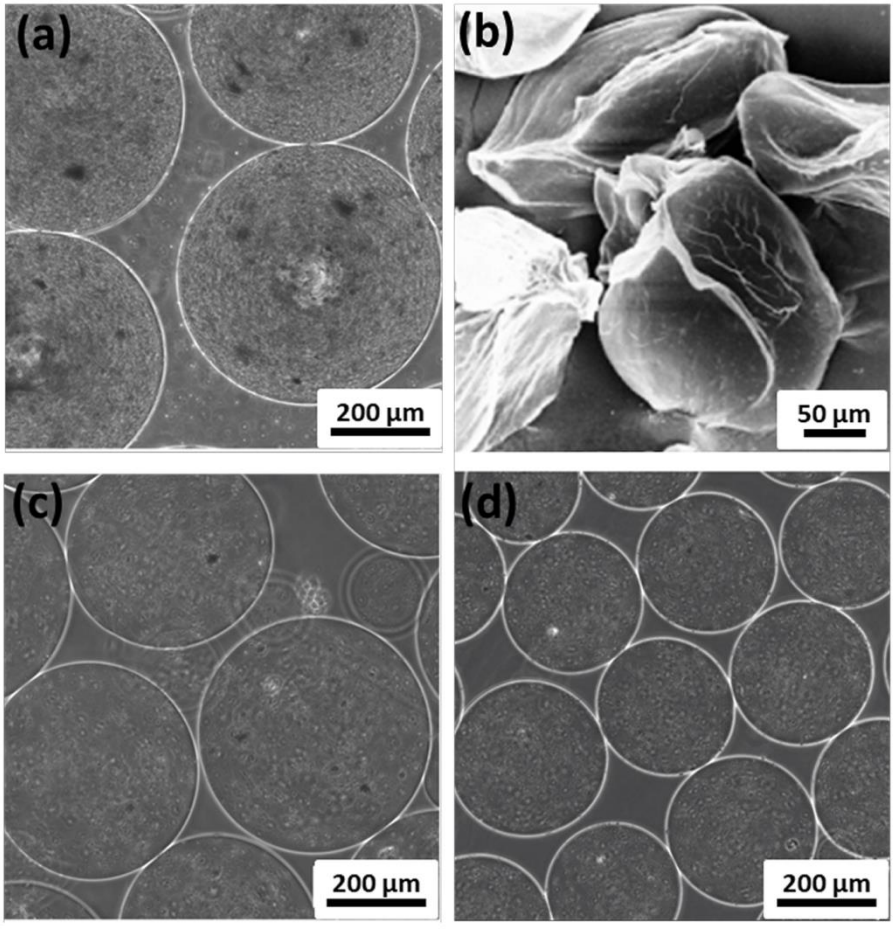

Figure S2. (a) Optical micrographs of 510 µm DM-ACMSs; (b) SEM image of DM-ACMSs; Optical micrographs of DM-ACMSs with different diameters of (c) 430 µm and (d) 290 µm.

S3. Preparation of amino-functionalized Fe_3O_4 nanoparticles (SPIONs-AED) and fluorescence labeling of Fe_3O_4 nanoparticles (SPIONs-AED-FITC)

The synthesis of FITC-labeled Fe_3O_4 nanoparticles (SPIONs-AED-FITC) was based on the reaction between the isothiocyanate group of FITC and the primary amino group of amino-functionalized nanoparticles (SPIONs-AED). The SPIONs-AED were prepared by conjugating cystamine onto water-soluble SPIONs through the -COOH group by using cross-linking reagents EDC and NHS. In this work, SPIONs (0.15mmol) were dissolved in monohydrate free acid solution (MES, pH=6), followed by the addition of EDC (1 mmol), the mixture was then stirred at room temperature for 15 min to activate the carboxylic group of nanoparticles. Subsequently, NHS (5 mmol) and cyst amine (0.75 mmol) in 25 mL PBS solution were added to the above solution, and the mixture was stirred for 2 h at room temperature. Excess EDC, NHS and cystamine were removed by centrifugation and the precipitation was washed three times with distilled water. Finally, SPIONs-AED were dispersed in water and stored at 4 ℃.

The SPIONs-AED-FITC was prepared by the addition of FITC into SPIONs-AED solutions. The FITC of 1 mg in 1 mL DMSO was diluted to PBS phosphate buffer solution to 50 μg/mL, which was added to 20 mL SPIONs-AED (8.5 mmol/L) aqueous solution followed by raising the pH to 8.8 with 0.5 mol/L NaOH. After 3 h of reaction in the dark at room temperature, the SPIONs-AED-FITC was washed with ethanol and separated by centrifuge until no fluorescence was detected in the supernatant. The SPIONs-FITC dissolved in PBS was stored at 4 ℃.

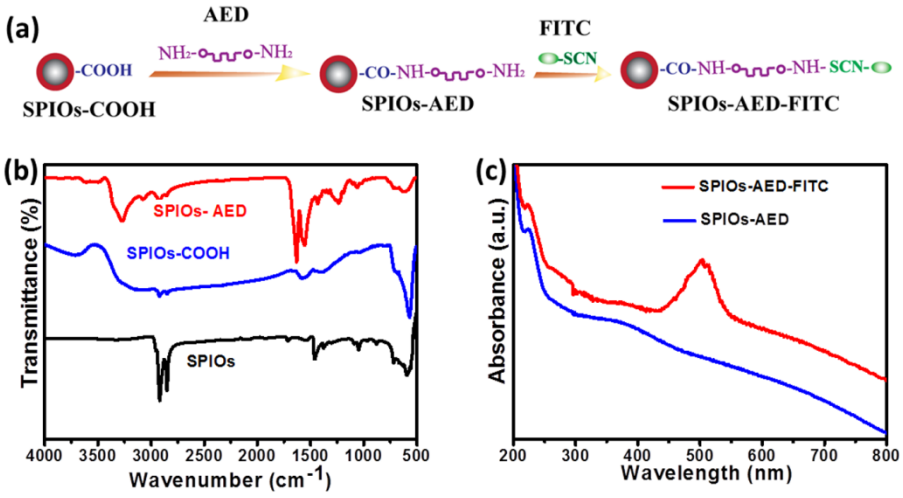

Figure S3. (a) Schematic illustration of the preparation procedure of SPIONs-AED-FITC; (b) FT-IR spectra of oleic acid coated SPIONs (SPIONs, black), after phase transfer (SPIONs-COOH, blue) and amino-functionalized SPIONs (SPIONs-AED, red); (c) UV-vis absorbance of SPIONs before (SPIONs-AED, blue) and after FITC labeled (SPIONs-AED-FITC, red).

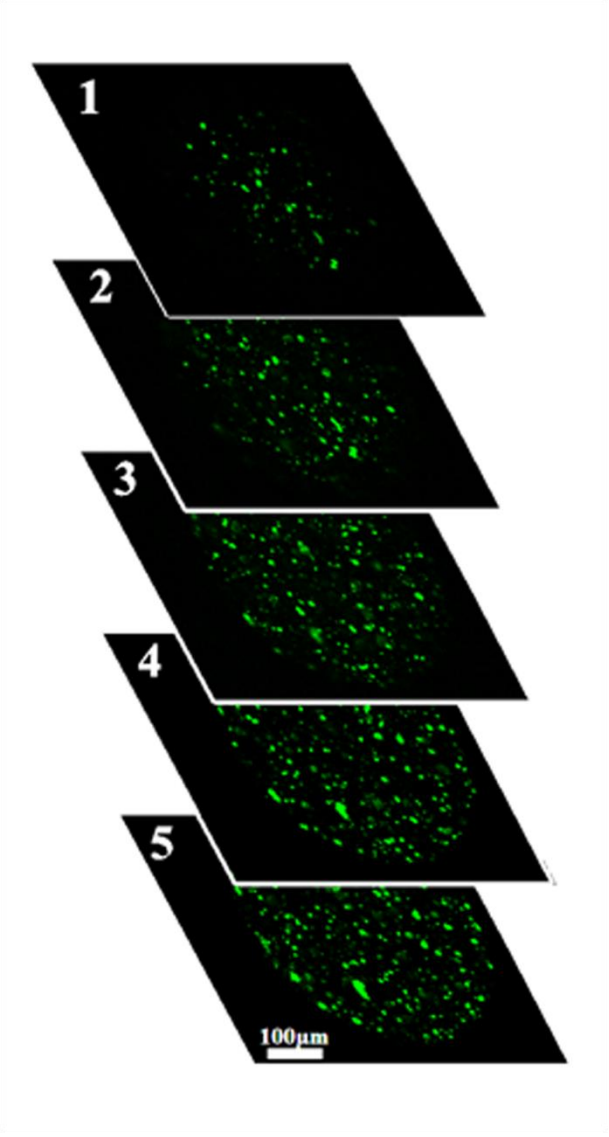

Figure S4. z-stack images of ACMSs with FITC-labeled SPIONs and DOX loaded. Depth increment is 34 μm.

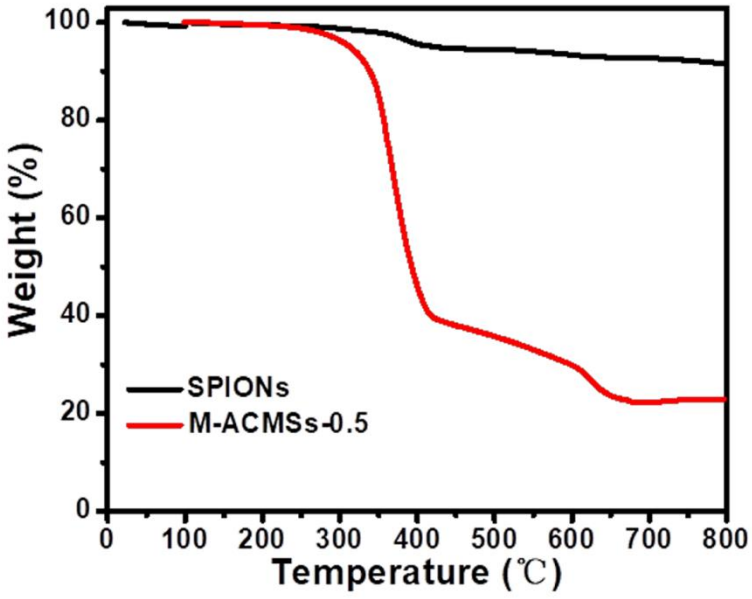

Figure S5. TGA profiles for SPIONs and M-ACMSs-0.5.

Table S1.The Fe loading ratio and SAR value for M-ACMSs with various concentrations (mg Fe/mL) of SPIONs loaded under an AMF (40 kA/m; 265 kHz).

	η_{SPION} (mg/g)	SAR value (W/g)
M-ACMSs-0.18	0.167	720.00±60.20
M-ACMSs-0.29	0.269	660.34±125.37
M-ACMSs-0.38	0.353	475.65±53.39
M-ACMSs-0.45	0.413	491.07±47.05
M-ACMSs-0.50	0.462	569.34±32.69

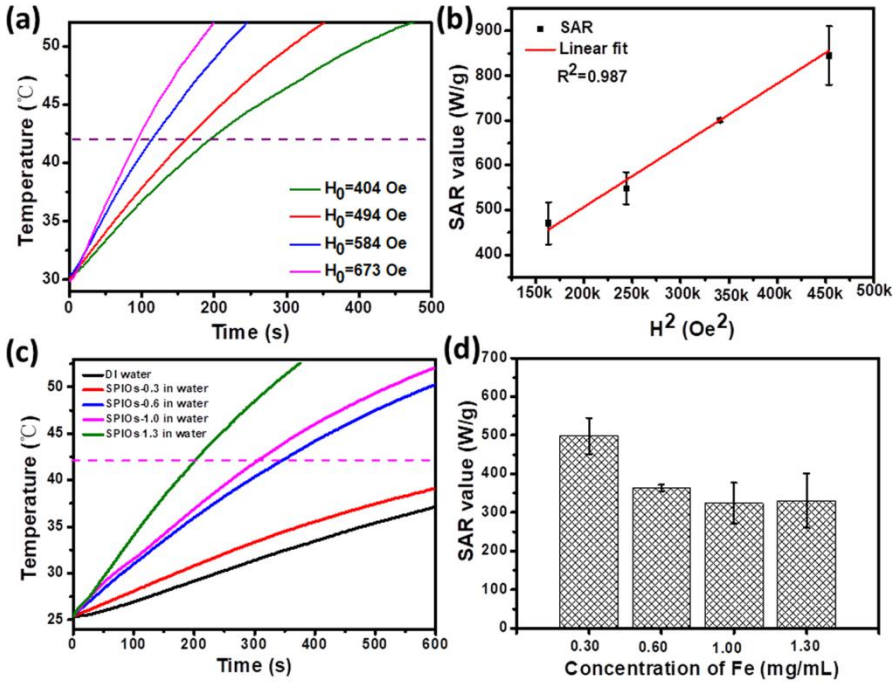

Figure S6. The time-dependent temperature rise (a) and SAR (b) for SPIONs loaded in ACMSs with Fe concentration of 0.50 mg/mL at different fields (H=404, 494, 584 and 673 Oe; f=265 kHz). The time-dependent temperature rise (c) and SAR (d) for various concentrations of SPIONs in water on exposure to 40 kA/m alternating current field at 265 kHz frequency;

Table S2 Summary of the properties of superparamagnetic Fe_3O_4 nanomaterials with their corresponding SAR, ILP values and AMF parameters.

	Core size	*Ms* (emu/g)	H (kA/m)	f (kHz)	SAR (W/g)	ILP (nHm^2/kg)	Reference
DM-ACMSs-0.29	510 μm	3	40	265	660	1.56	This study
SPIONs	14 nm	34	40	265	498	1.17	This study
FVIOs	70 nm	72	35	400	2213	4.52	1
Resovist	~10 nm	48	35	400	104	0.21	1
Fe_3O_4	~10 nm	64.54	15	300	168	2.49	2
Fe_3O_4	14 nm	75	24.5	400	447	1.86	3
Fe_3O_4	15 nm	~60	37.3	500	450	0.65	4
Fe_3O_4	9 nm	51	27	400	367	1.26	5
Fe_3O_4	9 nm	49	27	400	332	1.14	5
Fe_3O_4	9 nm	46	27	400	267	0.92	5
Fe_3O_4	19 nm	59	27	400	930	3.19	5
Fe_3O_4	19 nm	57	27	400	686	2.35	5
Fe_3O_4	19 nm	54	27	400	535	1.83	5

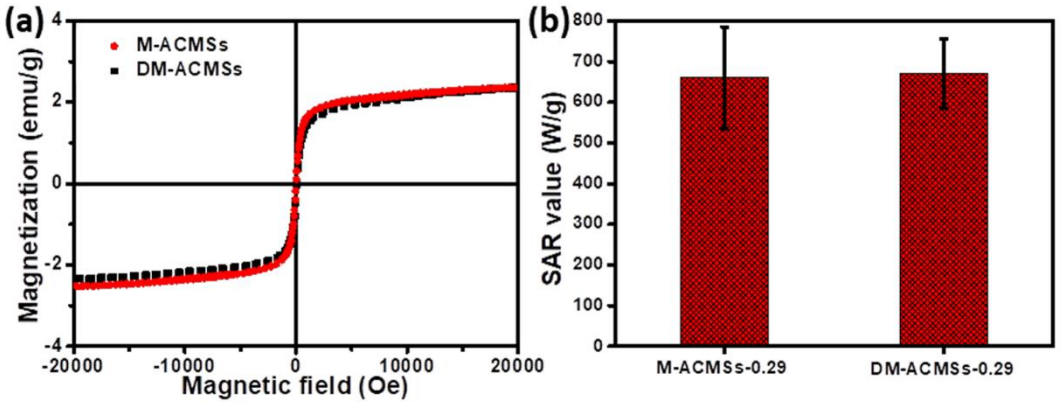

Figure S7. (a) VSM characterizations and (b) SAR value for M-ACMSs-0.29 and DM-ACMSs-0.29 under AMF (40 kA/m; 265 kHz).

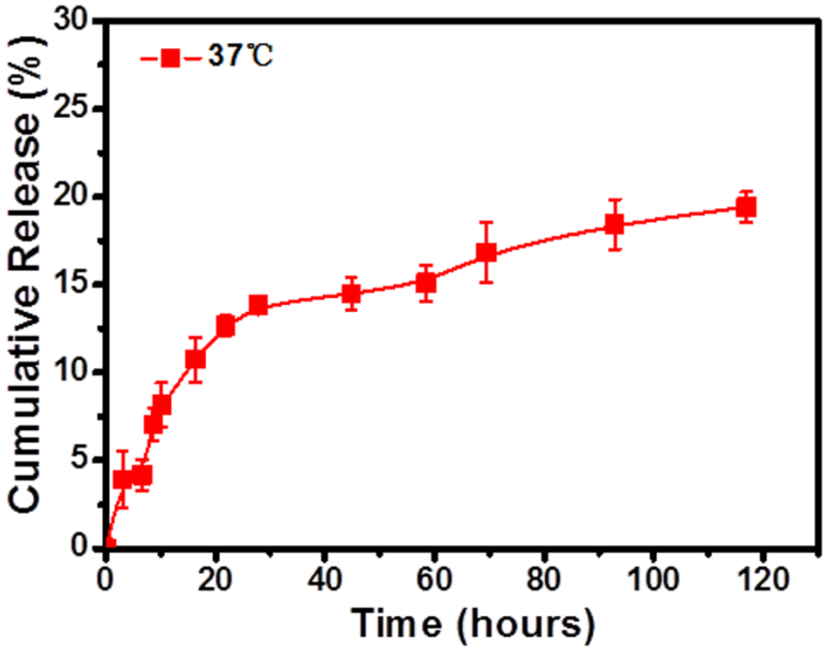

Figure S8. Cumulative release profile of DOX from ACMSs at 37℃.

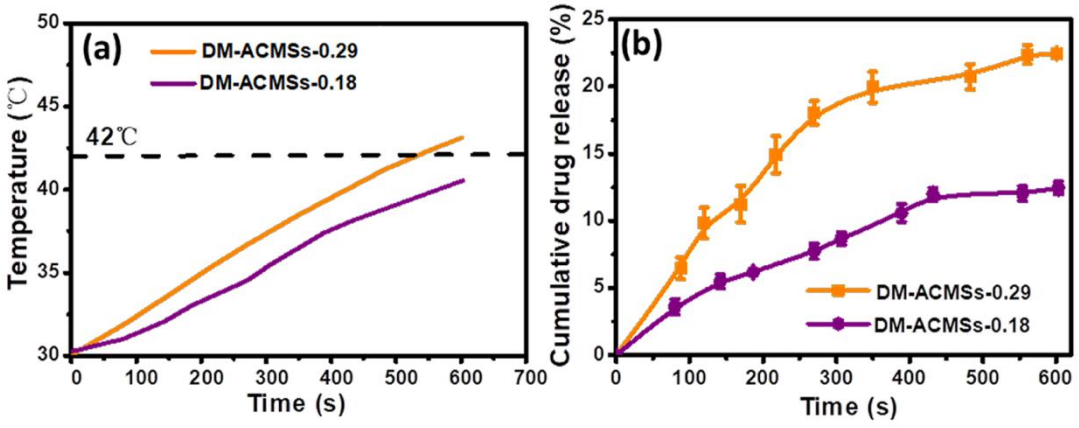

Figure S9. (a) T-t plot and (b) cumulative release profile of DOX for DM-ACMSs-0.18 and DM-ACMSs-0.29 under AMF (40 kA/m; 265 kHz).

Table S3. The DOX loading ratio (η_{DOX}) in DM-ACMSs with different concentration.

	DOX content in raw materials	**η_{DOX} (mg/g)**
DM-ACMSs-0.18	0.50 mg/mL	0.142
DM-ACMSs-0.29	0.50 mg/mL	0.149

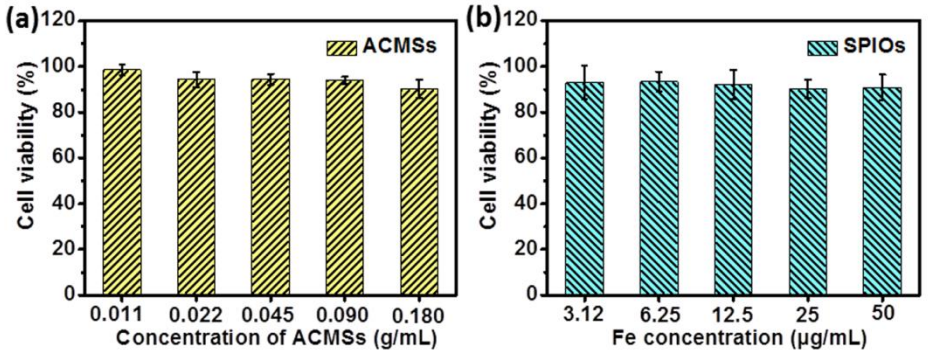

Figure S10. Cell viability of MCF-7 cells incubated with (a) ACMSs and (b) SPIONs at different concentrations for 24 h and recovered in fresh medium for 24 h.

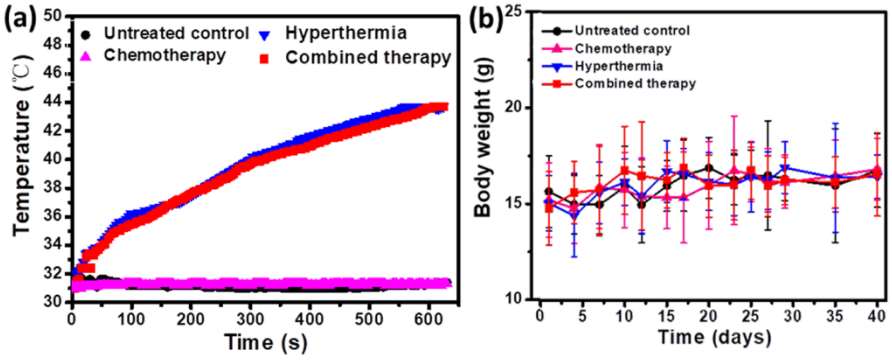

Figure S11. (a) Tumor temperatures change with different treatments; (b) The body weight of mice after treatment. The error bars represent the standard deviations (six mice per group).

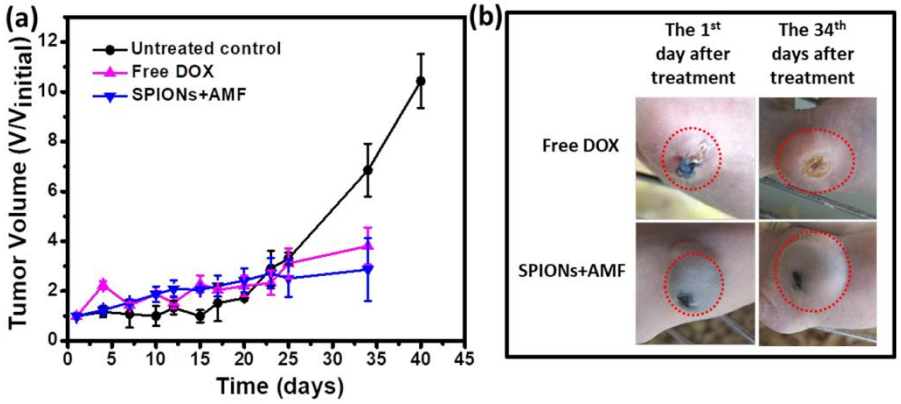

Figure S12. (a) Time-dependent changes of tumor volume for mice with different treatments. (b) *In vivo* evaluation of MCF-7 cells with chemo-thermal combination therapy.

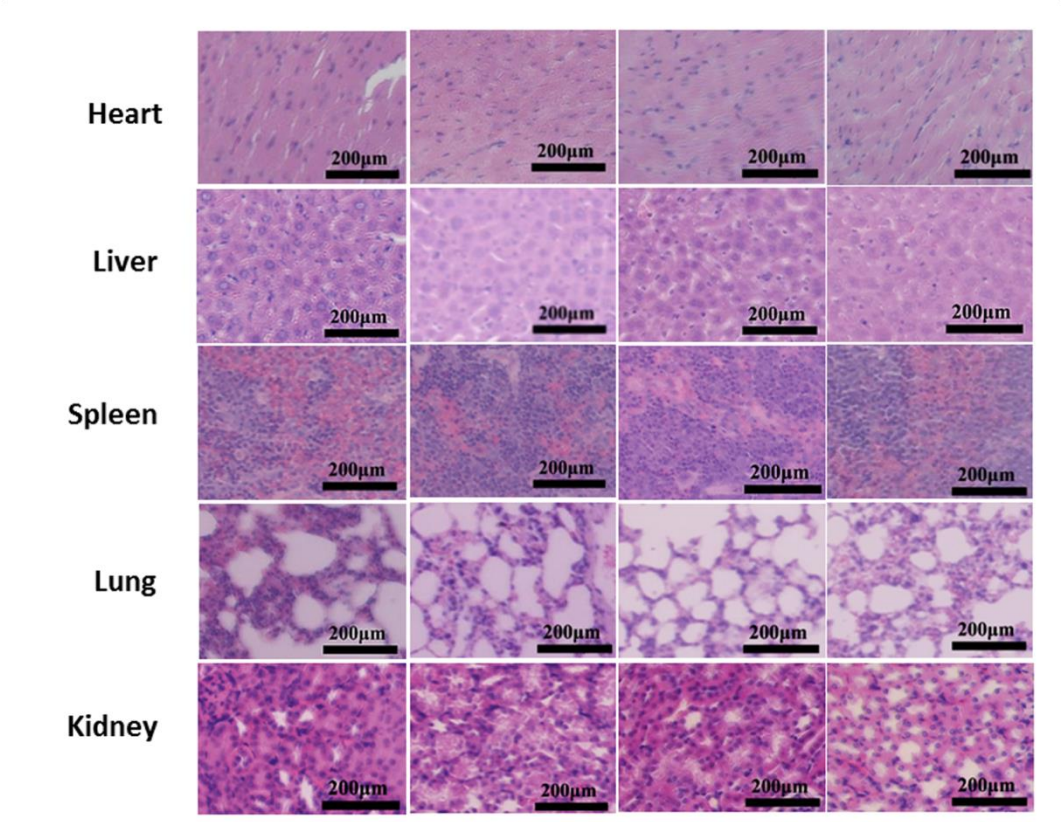

Figure S13. Histological evaluations of heart, lung, kidney, liver and spleen of mice with H&E staining.

References

[1] Liu X. L.; Yang Y.; Ng C. T.; Zhao L. Y.; Zhang Y.; Bay B. H.; Fan H. M.; Ding J. *Adv. Mater.* **2015**. 27, 1939-1944.

[2] Pradhan P.; Giri J.; Samanta G.; Sarma H. D.; Mishra K. P.; Bellare J.; Banerjee R.; Bahadur D. *J. Biomed. Mater. Res. B* **2007**. 81, 12-22.

[3] Gonzales-Weimuller M.; Zeisberger M.; Krishnan K. M. *J. Magn. Magn. Mater.* **2009**, 321, 1947-1950.

[4] Lee J. H.; Jang J. T.; Choi J. S.; Moon S. H.; Noh S. H.; Kim J. W.; Kim J. G.; Kim I. S.; Park K. I.; Cheon J. *Nat. Nanotechnol.* **2011**. 6, 418-422

[5] Liu X. L.; Fan H. M.; Yi J. B.; Yang Y.; Choo E. S. G.; Xue J. M.; Fan D. D.; Ding J. *J. Mater. Chem.* **2012**. 22, 8235.